0273-2289/99/77–79/0159/$12.50

Site-Directed Mutagenesis Study on the Thermal Stability of a Chimeric PQQ Glucose Dehydrogenase and Its Structural Interpretation

Arief Budi Witarto, Takafumi Ohtera, and Koji Sode*

Department of Biotechnology, Tokyo University of Agriculture and Technology, 2-24-16 Naka-machi, Koganei, Tokyo 184-8588, Japan, E-mail: sode@cc.tuat.ac.jp

Abstract

We have previously reported that a chimeric pyrroloquinoline quinone (PQQ) glucose dehydrogenase (GDH), E97A3, which was made up of 97% of *Escherichia coli* PQQGDH sequence and 3% of *Acinetobacter calcoaceticus* PQQGDH, showed increased thermal stability compared with both parental enzymes. Site-directed mutagenesis studies were carried out in order to investigate the role of amino-acid substitution at the C-terminal region, Ser771, of a chimeric PQQGDHs on their thermal stability. A series of Ser771 substitutions of a chimeric PQQGDH, E99A1, confirmed that hydrophobic interaction governs the thermal stability of the chimeric enzymes. Comparison of the thermal denaturation of *E. coli* PQQGDH and E97A3 followed by far-ultraviolet (UV) circular dichroism (CD) spectroscopy revealed that E97A3 acquired stability at the first step of denaturation, which is reversible, and where no significant secondary structure change was observed. These results suggested that the interaction between C-terminal and N-terminal regions may play a crucial role in maintaining the overall structure of β-propeller proteins.

Index Entries: PQQ glucose dehydrogenase; β-propeller protein; site-directed mutagenesis; CD spectroscopy; denaturation pathway.

Introduction

Many Gram-negative bacteria possess membrane-bound pyrroloquinoline quinone (PQQ) glucose dehydrogenase (GDH), which catalyze the oxidation of glucose into glucono-δ-lactone in the periplasm *(1)*. This enzyme is monomer with molecular weight of approx 87 kDa. Amino-acid

*Author to whom all correspondence and reprint requests should be addressed.

sequence analysis showed that PQQGDH is composed of two regions, a hydrophobic N-terminal region, thought to be important in anchoring the enzyme at inner-membrane, and a hydrophilic C-terminal region *(2)*. C-terminal region of PQQGDH has been predicted to fold into β-propeller structure *(3)*. β-propeller structure is composed of several sheets, which are formed by four anti-parallel β-strands called W-motif, arranged circularly like the blades of a propeller *(4)*. In all known β-propeller proteins, N-terminal and C-terminal are "joined" together either by hydrogen bonds, forming a sheet in the last W-motif of β-propeller structure with six to eight W-motif *(5–8)*, or by a disulfide bond, in the case of a β-propeller with four W-motif *(9)*.

PQQGDH has been attracted as a component of glucose sensor because it has high catalytic activity toward glucose and is not susceptible to oxygen interference like glucose oxidase, which is widely used in glucose sensors. We have been working on the protein engineering of PQQGDH in an attempt to improve enzymatic properties of the enzyme towards its application *(10–13)*. One of the approach is by constructing chimeric PQQGDHs by homologous recombination of *Escherichia coli* and *Acinetobacter calcoaceticus* PQQGDH structural genes, which differ in enzymatic properties. Among the chimeric PQQGDHs constructed, we found that one such chimera, E97A3, which is made up of a 97% *E. coli* PQQGDH sequence and a 3% *A. calcoaceticus* PQQGDH sequence, showed exceptional stability during purification and storage. E97A3 showed a more than 12-fold increase in half-life at 40°C compared with *E. coli* PQQGDH *(14)*. E97A3 has only three amino-acid substitutions (S771M, I786L, D794N) and one residue deletion (V801) compared with *E. coli* PQQGDH, all located in the last W-motif. On the other hand, another chimeric enzyme, E99A1, which has similar sequence with E97A3, except for having parental residue S771, showed reduced stability compared to *E. coli* PQQGDH. Thus, S771M mutation in E97A3 was suggested to be responsible for thermostability of the enzyme.

In order to investigate the strategy for thermostabilization of chimeric PQQGDH, site-directed mutagenesis at residue 771 was conducted and far-UV circular dichroism (CD) spectroscopy was employed to analyze the result from structural view. The denaturation pathway is also proposed.

Materials and Methods

Sample Preparation

Recombinant *E. coli* PQQGDH, chimera, and its mutants were expressed in *E. coli* PP2418 and purified as reported previously *(10,15)*.

Site-Directed Mutagenesis

Site-directed mutagenesis of PQQGDH was carried out using a plasmid vector pKF18k (Takara, Japan). *Ava*I–*Hin*dIII fragment of PQQGDH structural gene (*Ec*I) was subcloned into pKF18k. This plasmid was ther-

E99A1S771M	5'- GCC TGC **CAT** GAT CAC C -3'
E99A1S771Y	5'- GCC TGC **GTA** GAT CAC C -3'
E99A1S771F	5'- CC GCC TGC **GAA** GAT CAC C -3'
E99A1S771T	5'- GCC TGC **CGT** GAT CAC C -3'
E99A1S771E	5'- CC GTG ACC GCC TGC **TTG** GAT CAC CAC ATA C -3'
E99A1S771L	5'- GCC TGC **GAG** GAT CAC C -3'
E99A1S771Q	5'- CC GTG ACC GCC TGC **TTC** GAT CAC CAC ATA C -3'
E99A1S771P	5'- GCC TGC **GGG** GAT CAC C -3'
E99A1S771R	5'- GCC TGC **GCG** GAT CAC C -3'

Fig. 1. Oligonucleotide primers used for site-directed mutagenesis of E99A1 at S771. These oligonucleotides are complementary to nucleotides 2298–2327 of E99A1. Altered codons are bolded.

mally denatured to produce salmon-sperm (ss)DNA. The oligonucleotide primers used for mutagenesis at E99A1 S771M are shown in Fig. 1. According to the method of Hashimoto-Gotoh et al., plasmids harboring mutations were selected *(16)*. Mutation was then confirmed by automated DNA sequencer (Shimadzu, Kyoto, Japan). The *Ava*I–*Hin*dIII fragments were obtained and ligated with E99A1 digested by *Ava*I–*Hin*dIII, to construct an expression vector containing PQQGDH E99A1 mutants.

Thermal Inactivation

Thermal inactivation was measured by incubating enzyme solution in 10 m*M* potassium phosphate buffer, pH 7.0, containing 0.2% Triton X-100 at each temperature for a defined period. Samples were then stored at 4°C for 1 min. The residual enzyme activity was determined after holo-enzyme formation in 10 m*M* potassium phosphate buffer, pH 7.0, containing 0.2% Triton X-100, 10 m*M* $MgCl_2$ and 5 µ*M* PQQ for 1 h at 25°C. All enzyme assays were performed at room temperature. The first order rate constant, *k*, and half-life time of thermal inactivation ($t_{1/2}$) of irreversible thermal inactivation were obtained by linear regression in semilogarithmic coordinates at each temperature.

CD Spectroscopy

CD experiments were conducted using a J-720 spectropolarimeter (JASCO, Tokyo, Japan) with a Peltier type cell-holder, model PTC-343 (JASCO), which permits accurate temperature control. CD measurements were performed using 0.1-cm rectangular synthetic quartz cell with Teflon stopper, model S11-SQ-1 (GL Sciences, Tokyo, Japan). Protein concentrations were 200 µg/mL. CD temperature scans were performed by varying

the temperature from 25–95°C in a temperature slope of 50°C/h, and the ellipticity were measured at 197 nm with 0.2°C resolution, 4 s response time, and 1.0 nm bandwidth. The resulting curves were substracted with the data from buffer scan and then smoothed. CD wavelength scans were performed during the temperature scans using temperature-wavelength scan function of the incorporated JASCO software. CD spectra were measured from 260–190 nm with 0.2-nm intervals at the rate of 100 nm/min. A response time for each point was 2 s and the band width was 2.0 nm.

Secondary structure contents were predicted from each CD spectra using Convex Constraint Analysis (CCA) algorithm, which operates only on a collection of spectral data to extract the common spectral components with their spectral weights *(17)*. A collection of 30 membrane proteins CD spectra were used as reference of the deconvolution to distinguish transmembrane helix and peripheral helix *(18)*.

Results and Discussion

Role of Residue 771 in Thermal Stability

As reported previously, E97A3 showed up to 12-fold increased thermal stability, whereas E99A1 showed reduced thermal stability compared to *E. coli* PQQGDH *(14)*. Both chimeric enzymes have the same amino-acid sequence except for residue 771, which is methionine in E97A3 and serine in E99A1, as in the native *E. coli* PQQGDH. To test the possibility that mutation at residue 771 alone may greatly enhance thermal stability of PQQGDH, this residue in *E. coli* PQQGDH was substituted from serine to methionine (S771M). Thermal inactivation curve of *E. coli* PQQGDH S771M was compared with native *E. coli* PQQGDH, E97A3, and E99A1 (Fig. 2). In contrast to what was expected, thermal stability of *E. coli* PQQGDH S771M was in the same level with *E. coli* PQQGDH. Thus, point mutation at residue 771 alone could not increased the stability of *E. coli* PQQGDH and the effect of mutation at residue 771 is suggested to be specific to E99A1. To check this suggestion, residue 771 of E99A1 was substituted to several amino acids; hydrophobic amino acids, charged amino acids, and hydrophilic amino acids. Some of the typical results are shown in Fig. 3. Amino-acid substitutions at residue 771 of E99A1 resulted in a significant change of thermostability. E99A1 S771R was the most thermolabile mutant. Among the mutants obtained, E99A1 S771M, which has the same sequence with E97A3, acquired the highest thermostability in the same level with E97A3. These confirmed the effect of S771 mutation to thermostability is specific to E99A1.

All mutants constructed in this study were subjected to thermal inactivation at 40°C. Then their residual activities were measured. First-order rate constant and half-life time of thermal inactivation of all mutants are shown in Table 1. All charged and hydrophilic amino-acids mutations resulted in decreased half-life of the mutants indicating that neither ionic interaction nor hydrophilic residue is favorable. In contrast, except for leucine, amino acids with hydrophobicity greater than serine resulted in

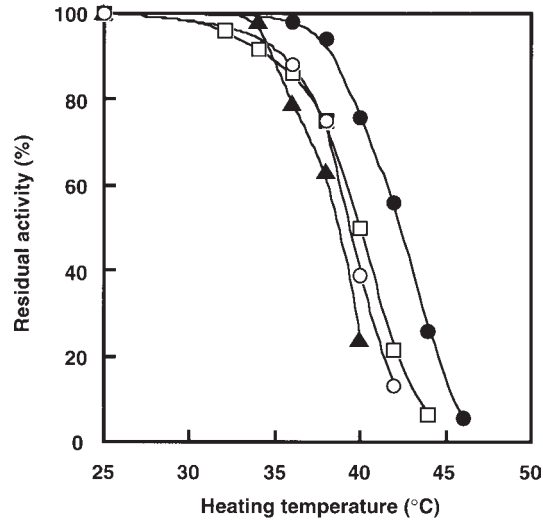

Fig. 2. Thermal inactivation of *E. coli* PQQGDH S771M compared with native *E. coli* and chimeric PQQGDHs. Residual activity of the apo-enzymes after 10-min incubation at each temperature were measured as described in Materials and Methods section. (●), E97A3; (▲), E99A1; (□), *E. coli* PQQGDH; (○), *E coli* PQQGDH S771M.

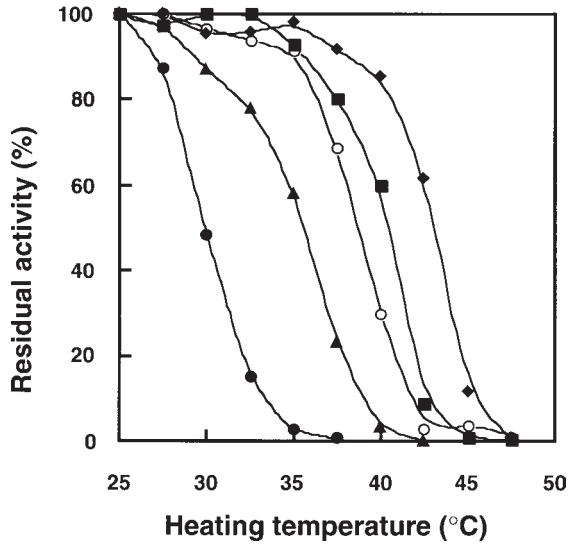

Fig. 3. Thermal inactivation of E99A1 S771 mutants. Residual activity of the apo-enzymes after 10-min incubation at each temperature were measured as described in Materials and Methods section. (●), E99A1 S771R; (▲), E99A1 S771L; (○), E99A1; (■), E99A1 S771F; (◆), E99A S771M.

increased half-life of thermal inactivation compared with E99A1 S771, indicating that hydrophobic interaction is responsible for the stability. Among the hydrophobic amino-acid mutations, S771M is the most

Table 1
First-Order Rate Constant and Half-Life Time
for Inactivation of E99A1 S771 Mutants at 40°C

	k(/s)	$t_{1/2}$ (min)
E. coli PQQGDH[a]	8.25×10^{-4}	14.00
S771M[a]	1.25×10^{-3}	9.24
E99A1S771M[b]	1.72×10^{-4}	67.30
E99A1S771Y[a]	6.35×10^{-4}	18.20
E99A1S771F[a]	9.98×10^{-3}	11.60
E99A1S771T[a]	1.15×10^{-3}	10.40
E99A1 (Ser771)[c]	2.01×10^{-3}	5.74
E99A1S771E[c]	3.28×10^{-3}	3.53
E99A1S771L[c]	3.27×10^{-3}	3.52
E99A1S771Q[c]	4.86×10^{-3}	2.38
E99A1S771P[c]	8.06×10^{-3}	1.43
E99A1S771R[c]	1.26×10^{-2}	0.92

Residual activity of the apo-enzymes were measured after incubation of: [a]2 min; [b]5 min, and [c]1 min.

thermostabile, whereas S771L showed less stability compared to S771. This might be a result of steric hindrance of the hydrophobic pocket, in which methionine fits well but can not accommodate leucine's bulky side-chain, yielding an unfavorable interaction.

Thermal Denaturation Pathway of PQQGDH

In order to analyze the structural stability of PQQGDH, thermal denaturation was carried out, followed by far-UV CD spectroscopy, which reflects the secondary structure of protein. *E. coli* PQQGDH was subjected to thermal denaturation by increasing the temperature gradually at a rate of 50°C/h and monitoring the ellipticity at 197 nm where largest ellipticity change was observed in the measurable wavelength. As shown in Fig. 4, PQQGDH showed three-step denaturation, from 30–40°C, 60–70°C, and 75–85°C. To analyze the conformation of PQQGDH at each denaturation step, CD spectra at 25, 50, 70, and 95°C were measured and the corresponding secondary structure contents were predicted. In order to distinguish transmembrane helix and peripheral helix, a CD spectrum analysis algorithm, CCA, which operates only on a collection of spectral data to extract the common spectral components with their spectral weights, was employed with a set of membrane proteins with CD spectra as reference *(18)*. As shown in Table 2, there is no difference in the content of transmembrane helix, which is consistent with the observation that the transmembrane helix commonly has high stability *(19)*. On the other hand, there is a remarkable change in the β-sheet content, which constitutes the majority of C-terminal region predicted to fold into β-propeller structure (Table 2). Although in the first step of denaturation from 30–40°C, large ellipticity

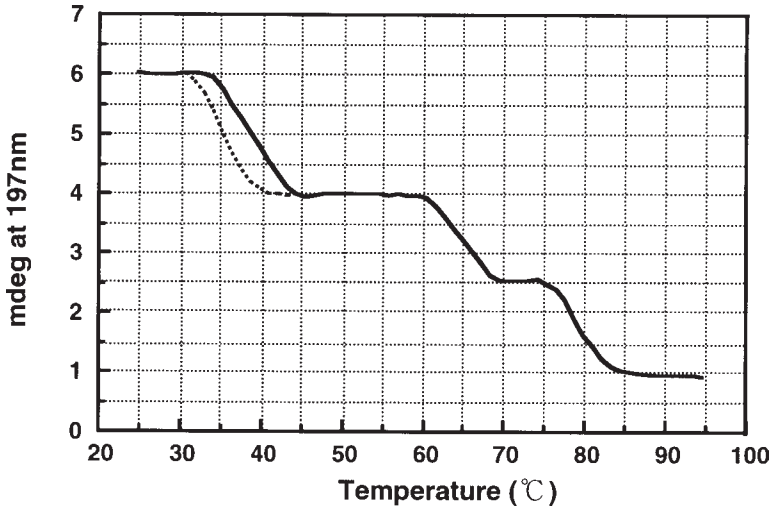

Fig. 4. Thermal denaturation of *E. coli* PQQGDH and E97A3. Thermal denaturations were followed by CD spectroscopy at 197 nm with protein concentration of 200 μg/mL, and cell pathlength of 0.1 cm. (—), *E. coli* PQQGDH; (⁻), E97A3.

Table 2
Secondary Structure Content of E97A3
at Each Temperature During Thermal Denaturation

Temperature	T_m-helix	Helix	Sheet	Turn	Random
25°C	17.5	4.0	35.2	7.0	36.3
50°C	17.2	3.3	33.4	8.1	38.0
70°C	17.4	2.8	22.8	14.2	42.8
90°C	17.0	1.2	11.5	20.6	49.7

changes were observed, indicating large conformational changes had occurred (Fig. 4), the secondary structures were only slightly altered, as shown by deconvolution of spectra obtained at 50°C (Table 2). After that, as shown by deconvolution of spectra obtained at 70 and 90°C, β-sheet content was gradually decreased, followed by increase in the content of random conformation (Table 2). Upon decreasing the temperature slowly from each temperature of the denaturation step, ellipticity after the first denaturation was restored to its initial value (data not shown). This suggest that the first denaturation is a completely reversible process. On the other hand, the second and third denaturation steps were not reversible.

To compare the thermal denaturation of *E. coli* PQQGDH and thermostable E97A3, a similar experiment was performed with E97A3. As shown in Fig. 4, E97A3 showed a similar denaturation curve. However, the first denaturation step of E97A3 was shifted to a higher temperature, indicating the E97A3 obtained stability at the first denaturation step. As in PQQGDH, the first step of denaturation of E97A3 is a reversible process, whereas the

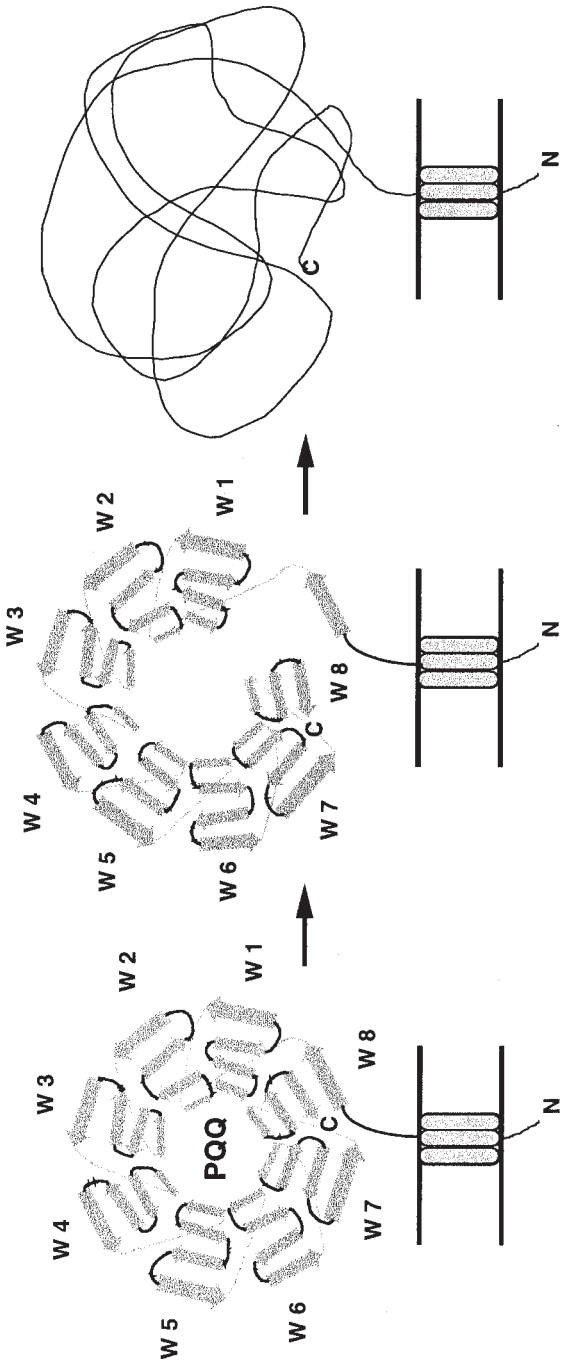

Fig. 5. Schematic model of the denaturation pathway of PQQGDH.

other two steps are not (data not shown). The first thermal denaturation step of *E. coli* PQQGDH and E97A3 between 30–45°C observed by CD (Fig. 4) indicates that a large conformation change occurred, but without remarkable secondary structure change as shown by deconvolution of CD spectra obtained at 25 and 50°C (Table 2), suggesting the formation of intermediate species. This intermediate species might be formed by the dissociation of interaction between N-terminal and C-terminal of β-propeller structure (Fig. 5). This suggestion is supported by the fact that E97A3, which differ in the C-terminal, acquired thermal stability in the first step of denaturation compared to PQQGDH. The next denaturation step is gradual denaturation of β-sheets of the β-propeller structure, as indicated by the decreased of β-sheet contents (Table 2).

C-terminal region of PQQGDH has been predicted to fold into a β-propeller structure, which consists of a PQQ binding site required for activity *(3)*. As shown in the site-directed mutagenesis study of E99A1 S771, increasing interaction between N-terminal and C-terminal of β-propeller domain is responsible for the improved stability. Thermal denaturation analyzed by CD spectroscopy analysis suggests that this interaction is crucial to maintaining the overall structure of β-propeller. Thus, improvement of the stability of PQQGDH might be achieved by enhancing the interaction between its N-terminal and C-terminal of β-propeller domain. Because, all β-propeller proteins known to date show this similar feature, this strategy might be applied to all β-propeller proteins.

Acknowledgments

The authors thank Dr. S. Ohuchi, K. Watanabe, and H. Yoshida for helpful discussions and assistance throughout the course of this study.

References

1. Matsushita, K. and Adachi, O. (1993), in *Principles and Applications of Quinoproteins*, Davidson, V. L. ed., Dekker, New York, pp. 47–63.
2. Cleton-Jansen, A. M., Goosen, N., Fayet, O., and van de Putte, P. J. (1990), *J. Bacteriol.* **172,** 6308–6315.
3. Cozier, G. E. and Anthony, C. (1995), *Biochem. J.* **312,** 679–685.
4. Murzin, A. G. (1992), *Proteins* **14,** 191–201.
5. Xia, Z., Dai, W., Xiong, J., Hao, Z., Davidson, V. L., White, S., and Mathews, F. S. (1992), *J. Biol. Chem.* **267,** 22,289–22,297.
6. Baker, S. C., Saunders, N. F. W., Willis, A. C., Ferguson, S. J., Hajdu, J., and Fulop, V. (1997), *J. Mol. Biol.* **269,** 440–455.
7. Wall, M. A., Coleman, D. E., Lee, E., Iniguez-Lluhi, J. A., Posner, B. A., Gilman, A. G., and Sprang, S. R. (1995), *Cell* **83,** 1047–1058.
8. Renault, L., Nassar, N., Vetter, I., Becker, J., Klebe, C., Roth, M., and Wittinghofer, A. (1998), *Nature* **392,** 97–101.
9. Li, J., Brick, P., O'hare, M. C., Skarzynski, T., Lloyd, L. F., Curry, V. A., Clark, I. M., Bigg, H. F., Hazleman, B. L., Cawston, T. E., and Blow, D. M. (1995), *Structure* **3,** 541–549.
10. Sode, K. and Sano, H. (1994), *Biotechnol. Lett.* **16,** 455–460.

11. Sode, K., Yoshida, H., Matsumura, K., Kikuchi, T., Watanabe, M., Yasutake, N., Ito, S., and Sano, H. (1995), *Biochem. Biophys. Res. Commun.* **211,** 268–273.
12. Sode, K., Shimakita, T., Ohuchi, S., and Yamazaki, T. (1996) *Biotechnol. Lett.* **18,** 997–1002.
13. Sode, K. and Kojima, K. (1997), *Biotechnol. Lett.* **19,** 1073–1077.
14. Sode, K., Watanabe, K., Ito, S., Matsumura, K., and Kikuchi, T. (1995), *FEBS Lett.* **364,** 325–327.
15. Sode, K., Witarto, A. B., Watanabe, K., Noda, K., Ito, S., and Tsugawa, W. (1994), *Biotechnol. Lett.* **16,** 1265–1268.
16. Hashimoto-Gotoh, T., Mizuno, T., Ogasahara, Y., and Nakagawa, M. (1995), *Gene* **152,** 271–275.
17. Perczel, A., Hollosi, M., Tusnady, G., and Fasman, G. D. (1991), *Protein Eng.* **4,** 669–679.
18. Park, K., Perczel, A., and Fasman, G. D. (1992), *Protein Sci.* **1,** 1032–1049.
19. Lau, F. W. and Bowie, J. U. (1997), *Biochemistry* **36,** 5884–5892.